Pressure-induced suppression of charge density wave and emergence of superconductivity in 1*T*-VSe_2

S. Sahoo,[1,2,*] U. Dutta,[1,2,*] L. Harnagea,[3] A. K. Sood,[4,†] and S. Karmakar[1,2,‡]

[1]*HP&SRPD, Bhabha Atomic Research Centre, Trombay, Mumbai 400085, India*

[2]*Department of Physical Sciences, Homi Bhabha National Institute, Anushaktinagar, Mumbai 400094, India*

[3]*Department of Physics, Indian Institute of Science Education and Research (IISER), Pune 411008, India*

[4]*Department of Physics, Indian Institute of Science, Bangalore 560012, India*

(Received 11 September 2019; revised manuscript received 15 January 2020; published 30 January 2020)

We report pressure evolution of charge density wave (CDW) order and the emergence of superconductivity (SC) in 1*T*-VSe_2 single crystal by studying resistance and magnetoresistance behavior under high pressure. With increasing quasihydrostatic pressure the CDW order enhances with its ordering temperature (∼100 K at ambient P) increasing marginally up to 5 GPa. At higher pressures, CDW-like resistance anomaly increases more rapidly with the characteristic temperature reaching ∼290 K at 14.2 GPa. Upon further increase of pressure, the resistance anomaly due to CDW order gets suppressed drastically with rapidly increased metallicity (as clearly evidenced from the increased RRR value) and superconductivity emerges at ∼15 GPa, with the onset critical temperature (T_c) ∼4 K. The pressure dependence of T_c is found negligible, different from an increase or a dome-shaped behavior seen in isostructural layered diselenide superconductors. The high-pressure magnetoresistance and Hall measurements suggest successive electronic structural changes with Fermi surface modifications at 5 and ∼12 GPa.

DOI: 10.1103/PhysRevB.101.014514

I. INTRODUCTION

Layered transition metal dichalcogenide (TMDC) compounds provide an ideal platform to explore exotic ground-state electronic orders by tuning the Fermi surface topology and many-body effects through various external stimulations [1]. Among these, 1*T*-structured correlated metals (e.g., 1*T*-TaS_2, 1*T*-$TaSe_2$, 1*T*-$TiSe_2$, and 1*T*-$TiTe_2$) have been extensively studied for understanding the mechanism of charge density wave (CDW) order at low temperature and its coexistence with superconductivity (SC) in some part of the phase diagram [2–8]. An unconventional (exciton or band-type Jahn-Teller) mechanism for the CDW ordering has been established in these compounds by several theoretical and experimental studies, rather than the conventional Fermi surface nesting mechanism [9–12]. However, the underlying mechanism for superconductivity is not conclusive so far. In some systems, the dome-shaped superconducting window in the vicinity of the CDW suppressed quantum critical point (QCP) supports unconventional SC scenario where CDW amplitude fluctuation is believed to be responsible for the Cooper pair formation [13–15]. In some other systems, phonon mediated (BCS type) SC appears in the phase diagram window (separated from the CDW region) that is believed to originate in phase-separated metallic domains [2,16].

1*T*-VSe_2 is one of the rare correlated metallic systems where three dimensional (3D) nesting of the Fermi surface gives rise to 3D-CDW ordering (having commensurate in-plane wave vector 0.25**a*** with an incommensurate out-of-plane component) [17–20]. The CDW transition temperature (T_{CDW}) is ∼110 K, as seen in resistivity and susceptibility measurements [21,22]. Due to weak nesting condition, the CDW distortion (amplitude) is small, making the superstructure bands not observable below T_{CDW} in ARPES measurements [18,19]. Although the high-resolution ARPES measurements on single crystal 1*T*-VSe_2 show the presence of only electron pocket (of V $3d_{z^2}$ band) at the *M* point of the Brillouin zone (BZ) as supported by the DFT calculations, the observed strong hybridization of Se $4p_{x,y}$ and $4p_z$ at the Γ point near the Fermi level [19] may turn the system into a multiband character by forming a $4p$ hole pocket. The Fermi surface topology thus appears to be very much susceptible to external perturbations like intercalation, reduced thickness or pressure to reveal exotic physical properties. While electron doping by alkali metal intercalation is found to alter the Fermi level band structure drastically into a 2D character [23,24], reduction of layer thickness shows anomalous change in the CDW ordering temperature due to dimensional crossover, reduced interlayer coupling and enhanced quantum confinement [25,26]. The study of monolayer VSe_2 has been of tremendous current interest as various synthesis procedures, substrate and strain conditions modify the Fermi surface drastically with emergence of different CDW order with distinct ordering temperatures, energy gap, Fermi arc and Mott/Peierls insulating state [27–30]. Monolayer VSe_2 has also been predicted to be energetically close to a

*These authors contributed equally to this work.

†asood@iisc.ac.in

‡sdak@barc.gov.in

spin-ordered structure [31], which has indeed been recently observed [32].

In spite of all these exotic physical properties, only very few investigations have so far been reported on the bulk $1T$-VSe_2 [21,22,33]. This is primarily due to the difficulties in the synthesis of pristine compound. It always grows as V-rich compound ($1T$-$V_{1+\delta}Se_2$) where extra V atoms are intercalated in the interlayer, giving rise to strong Curie-Weiss (CW) paramagnetic behavior at low temperature. These localized moments also act as Kondo scattering centres, which can also give rise to weak magnetic ordering at low temperature [22], hindering the study of intrinsic properties of $1T$-VSe_2. Here we report on the transport properties of $1T$-VSe_2 single crystal under high pressure. The in-plane resistance at room temperature shows anomalous pressure variation at ∼5 GPa, indicating change in its band structure and possibly the Fermi surface (FS) topology. With increasing quasihydrostatic pressure the CDW order enhances with its ordering temperature increasing marginally up to 5 GPa. At higher pressures, CDW-like resistance anomaly increases more rapidly with characteristic temperature reaching ∼290 K at 14.2 GPa. At further higher pressures the CDW-like feature is drastically suppressed and superconducting state emerges above 15 GPa. The SC T_c increases marginally with pressure, T_c reaching ∼5 K at 22 GPa, the highest pressure of our measurements. The low-temperature negative magnetoresistance (MR) due to Kondo scattering of interlayer V atoms is suppressed strongly above 12 GPa, consistent with corresponding vanishing of resistance upturn. The observed positive MR in the SC phase is typical of similar layered TMDCs. The Hall measurements further helps understand the FS modification under pressure leading to suppression of the CDW phase and emergence of SC. Upon decompression, significant resistance drop due to the onset of SC is observed down to 10 GPa, but without any sign of the coexistent CDW phase.

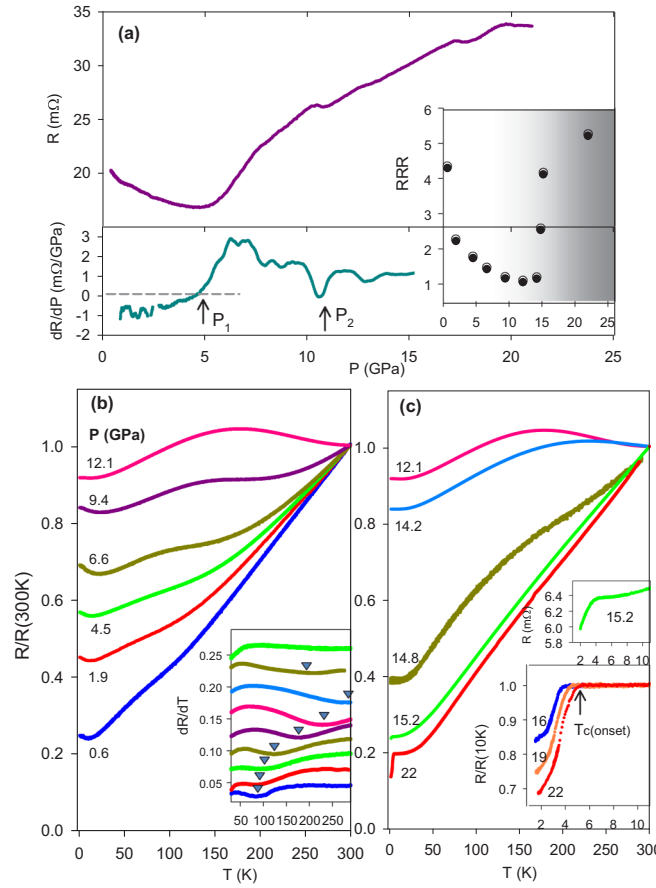

FIG. 1. (a) In-plane resistance of $1T$-VSe_2 at room temperature as a function of pressure. Lower panel displays the dR/dP vs P plot. [(b) and (c)] $R(T)/R(300\ \mathrm{K})$ are plotted as a function of temperature at various quasihydrostatic pressures. Inset in (b) shows the dR/dT plots at various pressures, the minima marked with down triangles indicate CDW transition temperatures. Insets in (c) show $R(T)$ at various pressures with onset of SC transition below 5 K.

II. EXPERIMENTAL

$1T$-$V_{1+\delta}Se_2$ (with $\delta \leqslant 0.03$) single crystals were grown by a conventional vapor transport method (with iodine as the transport agent) and characterized by x-ray diffraction, resistivity and magnetic susceptibility measurements (discussed in Ref. [34]). The resistance measurements were performed on the sample (dimension ∼120 μm × 100 μm × 5 μm, cut from a bigger crystal) using a standard four-probe technique (in van der Pauw configuration), with ac lock-in detection in two different high-pressure arrangements. A Stuttgart version diamond anvil cell (DAC) was used under quasihydrostatic pressure (up to 22 GPa) [35]. Finely ground NaCl powder was used as the pressure medium. A precalibrated motorized gear was used for pressure generation in a continuous mode at ∼0.2 GPa/min rate to study pressure variation of resistivity at room temperature. For measurements down to 1.4 K, the DAC was placed inside a KONTI-IT (Cryovac) cryostat, equipped with a homemade electromagnet coil (up to 0.5 T). For high-field measurements, a nonmagnetic Cu-Be DAC (M/s Easy Lab) was prepared for quasihydrostatic pressures (up to 15 GPa) and was inserted into a S700X SQUID magnetometer (M/s Cryogenic Ltd) to study MR and Hall resistance up to 7-T field and also dc susceptibility. Pressures were measured by conventional ruby luminescence.

III. RESULTS AND DISCUSSIONS

In Fig. 1(a), room-temperature in-plane resistance and its pressure derivative are shown as a function of pressure. The sample resistance initially decreases with increasing pressure up to ∼5 GPa (P1) where it starts increasing rapidly and at 22 GPa it becomes almost double, with two successive anomalies seen near ∼12 and ∼18 GPa. Although the system remains metallic over the entire pressure range, the rapid upturn at 5 GPa showing emergence of additional scattering channels indicates significant modification of band structure near Fermi level.

Figures 1(b) and 1(c) show temperature variation of the $R(T)/R(300\ \mathrm{K})$ curves under various quasihydrostatic pressures up to 22 GPa. The lowest pressure (0.6 GPa) R-T plot agrees well with the one at ambient pressure [34]. Although the CDW anomaly near 110 K is not as pronounced as observed from larger single crystal, the ordering temperature can be unambiguously determined from the minimum of dR/dT

curve [inset of Fig. 1(b)] [10,25]. A clear resistance upturn below 10 K is identified as due to Kondo effect arising from the scattering of conduction electrons by interlayer V ions localized magnetic moments. The CW-fitted susceptibility [34] verifies slightly higher level of V ion concentration in our sample than that reported in Ref. [22], agreeing with slightly lower CDW transition temperature and higher Kondo temperature. With increasing pressure, the CDW feature in resistance is enhanced with higher ordering temperature with a change in pressure derivative of T_{CDW} at ~5 GPa, supporting the FS modification at this pressure as discussed above. The pressure-driven rapid increase of CDW ordering is rather unusual. For further evidence of CDW ordering, high-pressure measurements using direct techniques are necessary. The broad resistance anomaly indicates the emergence of new electronic phase at low T with reconstructed Fermi surface where CDW ordering could be one of the possible mechanisms for the resistance anomaly and dR/dT minima can be ascribed as its characteristic temperature. Also the residual resistance ratio (RRR $= R_{300\,K}/R_{10\,K}$) rapidly decreases from ~4.4 to ~1 at 12 GPa, indicating rapidly decreased metallic character [inset in Fig. 1(a)]. At a higher pressure (14.2 GPa), while the hump like resistance anomaly moves to further higher temperature, the RRR value increases. At further higher pressures, this resistance anomaly drastically disappears, with rapid increase in RRR showing enhanced metallic character [Fig. 1(c)]. At 15.2 GPa, a significant resistance drop below 4 K indicates the onset of SC transition [upper inset of Fig. 1(c)]. The resistance drop increases with increasing pressure with marginal increase of onset T_c, reaching ~5 K at 22 GPa. As the SC state emerges at a pressure where resistance anomaly (due to reconstructed Fermi surface with possibilities of CDW ordering) completely gets suppressed, we conclude that SC and CDW do not coexist. Throughout the pressure range SC transition is not complete at the lowest T (1.4 K) of our set up and hence zero resistance is not achieved in four-probe resistance measurements (even from repeated loading) due to the intrinsic broad transition width [lower inset of Fig. 1(c)]. An incomplete SC transition in this system can be attributed to the presence of interlayer Kondo impurities [36]. Also we believe a post-growth treatment of the sample may help remove strain/defects and bring the sample close to the ideal stoichiometry that may increase the superconducting volume fraction and sharpen the transition. Upon releasing pressure, the resistance drop due to onset SC is seen down to 10 GPa with enhanced T_c (Fig. 7s top right panel in Ref. [34]).

In Fig. 2(a), we plot the magnetic field variation of $R(T)$ at 15.2 GPa around T_c. The resistance drop (with zero field onset T_c ~ 4 K) is gradually lifted with increasing field, resulting in a systematic decrease in T_c. At a magnetic field of 1.5 T, the SC transition almost smears out. In all our four-probe resistance measurements, we observed partial resistance drop down to 1.4 K (even with lowest applied current, Fig. 6s in Ref. [34]). The significant broad transition is believed to be intrinsic due to the presence of localized magnetic moments. In order to verify the SC nature, we performed DAC based dc-susceptibility measurements where significant diamagnetic drop is noticed below 3.2 K [inset of Fig. 2(a)]. Although the bulk nature is verified, the SC shielding fraction is small (of filamentary nature) in absence of zero resistance. A field

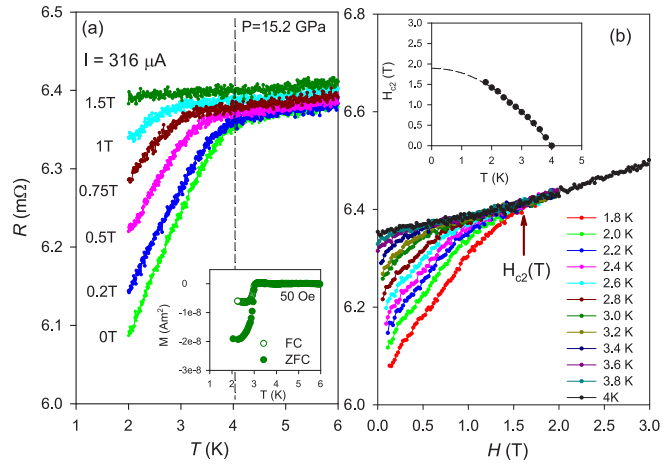

FIG. 2. (a) R-T data near SC onset T_c at 15 GPa under different fields up to 1.5 T. Inset shows field cooled and zero-field cooled dc-susceptibility data at 50 Oe field from the sample pressurized at 15 GPa. (b) Field scanning of low-temperature resistance $R(H)$ below SC T_c to determine the upper critical field of the SC emerged at 15 GPa. Inset shows the $H_{c2}(T)$ plots at various T below T_c and the GL-fitted curve.

direction dependent measurement would be necessary to further understand the SC properties in this layered compound. In order to find the upper critical field, we have performed field scanning measurements at various low temperatures below T_c [shown in Fig. 2(b)]. In the T-H_{c2} plot [inset of Fig. 2(b)], when fitted with Ginzburg-Landau (GL) formula (for BCS SC) gives $H_{c2}(0) = 1.9$ T, agreeing very well with the observation in typical layered TMDC.

To understand the evolution of electronic structure exhibiting SC, we carried out magnetoresistance (MR) and Hall measurements at high P (up to 7-T field along the c axis). In Fig. 3, we plot the temperature dependence of MR at 7-T field $MR(\%)$ $[=(R_{7\,T} - R_{0\,T})\times\ 100/R_{0\,T}]$ at various quasihydrostatic P. While the zero field Kondo scattering resistance upturn increases with pressure (Fig. 4s in Ref. [34]), the negative MR (the signature of scattering through magnetic moments) systematically decreases (red squares in inset of Fig. 3). This is due to the fact that an applied 7-T field ($H < H_K = k_B T_K/\mu$ where localized moment $\mu = 2.5\ \mu_B$) is able to suppress this scattering only partially causing a reduced negative MR (as discussed in Ref. [34]). At low pressures, a small positive MR is observed above T_{Kondo} as reported earlier [22]. However, at 4.5 GPa, this MR becomes negative over broad T range, which is much enhanced at 6.6 GPa (Fig. 3). Such negative MR can be attributed to the spin dependent scattering possibly due to emergence of the short range antiferromagnetic interaction in triangular V lattice [32,37]. At further higher pressure (9.4 GPa). the MR reverses its sign and a positive MR reappears. The CDW state above T_{Kondo} thus passes through a large negative MR at ~5 GPa (inset of Fig. 3), indicating dramatic change in its band structure, supporting the anomalous pressure dependence of room temperature resistance at this pressure [Fig. 1(a)]. Figure 4(a) displays the suggested electronic phase diagram of 1T-VSe_2 from our measurements. The CDW ordering temperature gets enhanced immediately

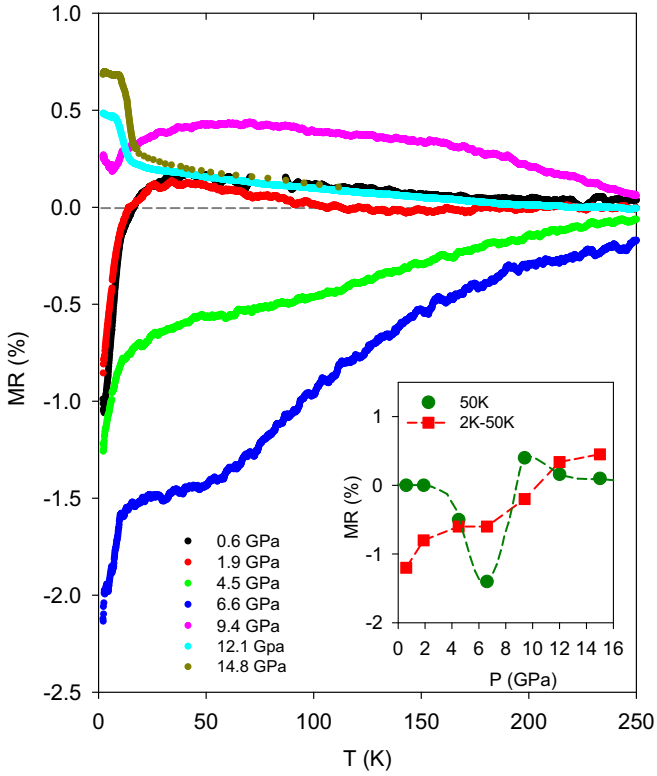

FIG. 3. T-dependent in-plane magnetoresistance at 7-T field applied along c axis, $MR(\%)$ $[=(R_{7T}-R_{0T})\times 100/R_{0T}]$ at various quasihydrostatic P. Inset shows the pressure dependence of MR at 50 K (green) and at 2 K (red, after subtracting the CDW state contribution at 50 K).

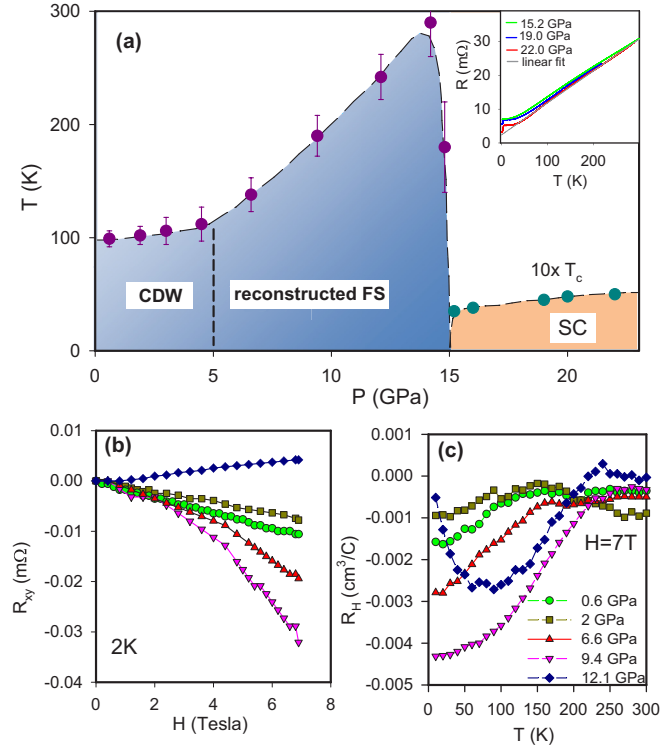

FIG. 4. (a) $P-T$ electronic phase diagram of $1T$-VSe_2 showing pressure evolution of CDW ordering T as well as SC T_c. Inset shows overall linear $R(T)$ behavior above SC T_c for $P > 15$ GPa (b) In-plane transverse MR with zero correction (Hall resistance R_{xy}) at 2 K as a function of applied magnetic field along c axis and (c) Hall coefficient, R_H $(=R_{xy}/H$ at 7-T field) as a function of T at various pressures.

after this band structure modification (probably by achieving better FS nesting condition), also supported by increased pressure derivative of T_{CDW} at this pressure. In absence of any direct evidence of the CDW order at higher pressures, we mark this new electronic phase with "reconstructed Fermi surface" in the phase diagram. At low pressures (<5 GPa), relatively smaller pressure coefficient of T_{CDW} in comparison with the reported result [33] might be due to the quasihydrostatic pressure medium in our measurement. Interestingly, as shown in inset of Fig. 4(a), the linear T dependence of $R(T)$ is observed down to ~30 K, much below the reported Debye temperature (~220 K [38,39]), indicating a non-Fermi liquid (nFL) behavior above the SC dome (as commonly seen in cuprate high temperature superconductors). This suggests for an unconventional nature of superconductivity emerging at high pressure in VSe_2.

The rapid electronic structural modification is further evidenced from our high-pressure Hall measurements. Figure 4(b) shows P dependence of the in-plane transverse magnetoresistance (R_{xy}) measured at 2 K as a function of magnetic field applied along c axis. The negative R_{xy} and its linear field dependence at low pressures agree very well with the reported results [22,25]. In the low-P range (below 5 GPa), upon increasing P, R_{xy} slope decreases, indicating the enhanced carrier concentration. However, at 6.6 GPa, we see a reverse trend, R_{xy} slope starts increasing and strong nonlinear field dependence is observed at high field, which becomes further enhanced at 9.4 GPa. This clearly indicates a transition from single band to multiband carrier behavior. The pressure-induced change in carrier behavior is also apparent from the Hall coefficient (at 7-T field) plots as a function of temperature [Fig. 4(c)]. At 0.6 GPa, with lowering T below CDW ordering a rapid increase of negative R_H is noticed due to reduced carrier concentration ($n \propto 1/R_H$) as a result of partial gapping near Fermi level. In the low-P range ($P <$ 5 GPa), overall carrier concentration systematically increases due to increased $3d_{z^2}$ bandwidth. However, for $P > 5$ GPa, a rapid overall increase of negative R_H is observed with large positive shift of T_{CDW}. The pressure-induced anomalous change in Hall coefficient is presumably due to emergence of small hole pocket (derived from Se $4p$ orbitals) at the Γ point of the BZ, supporting the nonlinear field dependence of R_{xy}.

At 12 GPa we further observe a drastic change in Hall resistance behavior; R_{xy} at 2 K becomes positive, indicating dominating hole contribution near Fermi level. A drastic change of the RRR value above 12 GPa [inset in Fig. 1(a)] further supports the rapid modification of band structure near Fermi level. Moreover, T-dependent Hall coefficient at this pressure shows dramatic change in carrier concentration [Fig. 4(c)]. Upon lowering temperature R_H increases as a result of CDW ordering, but sharply decreases below 100 K and changes sign below 10 K. This is clear from the positive field dependent R_{xy} at 2 K [Fig. 4(b)], suggesting

hole-dominated transport at this pressure. From Fig. 3, we see that at 12 GPa, while MR at higher T still remains at a small positive value, at low T, significantly large positive MR appears in the much suppressed Kondo scattering regime. At further higher pressures this positive MR persists at low temperature (Fig. 5s of Ref. [34]). A small positive MR is a common feature of non-CDW phase in pristine and pressurized layered TMDCs, originating from electron cyclotron orbital effect due to the Lorentz force [7,10,37]. However, the large positive MR below 10 K can be due to the enhanced exchange interaction of reminiscent localized moments at this pressure. Further field dependent measurements are needed to confirm its magnetic origin. The signatures of much enhanced metallic character with abrupt change in carrier behavior indicate dramatic changes in the electronic band structure above 12 GPa. A structural transition is not ruled out at this pressure which warrants detailed high-pressure x-ray diffraction investigations [40].

The Kondo resistance upturn is found to shift to higher T (with increased Kondo temperature) with increasing pressure up to 9.4 GPa, beyond which it decreases and eventually vanishes in the resistance data at 14.8 GPa, (Figs. 4s and 5s in Ref. [34]). Increased Kondo scattering at higher P is attributed to the increased effective exchange interaction between localized moments and/or enhanced density of state (DOS) at Fermi level of the host VSe_2 [41,42]. However, as CDW order is enhanced, the metallic character decreases upon increasing P, with reduced DOS and therefore increased exchange interaction responsible for increased Kondo temperature.

IV. CONCLUSION

In conclusion, 1T-VSe_2 single crystals show pressure-induced significant changes in electronic structure resulting in change in CDW ordering at ∼5 GPa and subsequently dramatic suppression of CDW phase above 12 GPa. Pressure-induced onset of SC transition ($T_c \sim 4$ K) is observed above 15 GPa. The SC T_c marginally increases with pressure up to 22 GPa. The non-dome-shaped feature as well as low-overlapping region with CDW phase rule out the real space co-existence of the two quantum electronic order. The measured upper critical field is of the same order as in isostructural layered diselenide superconductors. The high-pressure magnetoresistance and Hall measurements suggest successive electronic structural changes with Fermi surface modifications at ∼5 and 12 GPa. Further high-pressure investigations are to be performed to understand the CDW phase diagram as well as the nature of SC.

ACKNOWLEDGMENTS

A.K.S. thanks Department of Science and Technology for financial assistance. L.H. acknowledges Department of Science and Technology, India [Grant No. SR/WOS-A/PM-33/2018 (G)] for funding support and Prof. Surjeet Singh for allowing the use of his crystal growth facilities.

[1] A. V. Kolobov and J. Tominaga, *Two-dimensional Transition Metal Dichalcogenides*, Springer Series in Material Science Vol. 239 (Springer, Switzerland, 2016).
[2] B. Sipos, A. F. Kusmartseva, A. Akrap, H. Berger, L. Forró, and E. Tutis, Nat. Mater. **7**, 960 (2008).
[3] R. Ang, Y. Tanaka, E. Ieki, K. Nakayama, T. Sato, L. J. Li, W. J. Lu, Y. P. Sun, and T. Takahashi, Phys. Rev. Lett. **109**, 176403 (2012).
[4] B. Wang, Y. Liu, K. Ishigaki, K. Matsubayashi, J. Cheng, W. Lu, Y. Sun, and Y. Uwatoko, Phys. Rev. B **95**, 220501(R) (2017).
[5] E. Morosan, H. W. Zandbergen, B. S. Dennis, J. W. G. Bos, Y. Onose, T. Klimczuk, A. P. Ramirez, N. P. Ong, and R. J. Cava, Nat. Phys. **2**, 544 (2006).
[6] A. F. Kusmartseva, B. Sipos, H. Berger, L. Forró, and E. Tutiš, Phys. Rev. Lett. **103**, 236401 (2009).
[7] U. Dutta, P. S. Malavi, S. Sahoo, B. Joseph, and S. Karmakar, Phys. Rev. B **97**, 060503(R) (2018).
[8] U. Dutta, S. Sahoo, P. S. Malavi, F. Piccirilli, P. Di Pietro, A. Perucchi, S. Lupi, and S. Karmakar, Phys. Rev. B **99**, 125105 (2019).
[9] W. Kohn, Phys. Rev. Lett. **19**, 439 (1967).
[10] F. J. D. Salvo, D. E. Moncton, and J. V. Waszczak, Phys. Rev. B **14**, 4321 (1976).
[11] K. Rossnagel, L. Kipp, and M. Skibowski, Phys. Rev. B **65**, 235101 (2002).
[12] T. E. Kidd, T. Miller, M. Y. Chou, and T.-C. Chiang, Phys. Rev. Lett. **88**, 226402 (2002).
[13] H. Barath, M. Kim, J. F. Karpus, S. L. Cooper, P. Abbamonte, E. Fradkin, E. Morosan, and R. J. Cava, Phys. Rev. Lett. **100**, 106402 (2008).
[14] Y. I. Joe, X. M. Chen, P. Ghaemi, K. D. Finkelstein, G. A. de la Peña, Y. Gan, J. C. T. Lee, S. Yuan, J. Geck, G. J. MacDougall, T. C. Chiang *et al.*, Nat. Phys. **10**, 421 (2014).
[15] A. Kogar, G. A. de la Pena, S. Lee, Y. Fang, S. X.-L. Sun, D. B. Lioi, G. Karapetrov, K. D. Finkelstein, J. P. C. Ruff, P. Abbamonte, and S. Rosenkranz, Phys. Rev. Lett. **118**, 027002 (2017).
[16] Y. Liu, D. F. Shao, L. J. Li, W. J. Lu, X. D. Zhu, P. Tong, R. C. Xiao, L. S. Ling, C. Y. Xi, L. Pi *et al.*, Phys. Rev. B **94**, 045131 (2016).
[17] K. Tsutsumi, Phys. Rev. B **26**, 5756 (1982).
[18] K. Terashima, T. Sato, H. Komatsu, T. Takahashi, N. Maeda, and K. Hayashi, Phys. Rev. B **68**, 155108 (2003).
[19] V. N. Strocov, M. Shi, M. Kobayashi, C. Monney, X. Wang, J. Krempasky, T. Schmitt, L.Patthey, H. Berger, and P. Blaha, Phys. Rev. Lett. **109**, 086401 (2012).
[20] W. Jolie, T. Knispel, N. Ehlen, K. Nikonov, C. Busse, A. Grüneis, and T. Michely, Phys. Rev. B **99**, 115417 (2019).
[21] C. F. van Bruggen and C. Haas, Solid State Commun. **20**, 251 (1976).
[22] S. Barua, M. C. Hatnean, M. R. Lees, and G. Balakrishnan, Sci. Rep. **7**, 10964 (2017).
[23] H. I. Starnberg, H. E. Brauer, L. J. Holleboom, and H. P. Hughes, Phys. Rev. Lett. **70**, 3111 (1993).

[24] H. E. Brauer, H. I. Starnberg, L. J. Holleboom, V. N. Strocov, and H. P. Hughes, Phys. Rev. B **58**, 10031 (1998).
[25] J. Yang, W. Wang, Y. Liu, H. Du, W. Ning, G. Zheng, C. Jin, Y. Han, N. Wang, Z. Yang *et al.*, Appl. Phys. Lett. **105**, 063109 (2014).
[26] A. Pasztor, A. Scarfato, C. Barreteau, E. Giannini, and C. Renner, 2D Mater. **4**, 041005 (2017).
[27] D. Zhang, J. Ha, H. Baek, Y.-H. Chan, F. D. Natterer, A. F. Myers, J. D. Schumacher, W. G. Cullen, A. V. Davydov, Y. Kuk *et al.*, Phys. Rev. Materials **1**, 024005 (2017).
[28] P. Chen, W. W. Pai, Y.-H. Chan, V. Madhavan, M. Y. Chou, S.-K. Mo, A.-V. Fedorov, and T.-C. Chiang, Phys. Rev. Lett. **121**, 196402 (2018).
[29] G. Duvjir, B. K. Choi, I. Jang, S. Ulstrup, S. Kang, T. T. Ly, S. Kim, Y. H. Choi, C. Jozwiak, A. Bostwick *et al.*, Nano Lett. **18**, 5432 (2018).
[30] Y. Umemoto, K. Sugawara, Y. Nakata, T. Takahashi, and T. Sato, Nano Res. **12**, 165 (2019).
[31] M. Esters, R. G. Hennig, and D. C. Johnson, Phys. Rev. B **96**, 235147 (2017).
[32] P. K. J. Wong, W. Zhang, F. Bussolotti, X. Yin, T. S. Herng, L. Zhang, Y. L. Huang, G. Vinai, S. Krishnamurthi, D. W. Bukhvalov *et al.*, Adv. Mater. **31**, 1901185 (2019).
[33] R. H. Friend, D. Jerome, D. M. Schleich, and P. Molinie, Solid State Commun. **27**, 169 (1978).
[34] See Supplemental Material at http://link.aps.org/supplemental/10.1103/PhysRevB.101.014514 for synthesis, characterization by x-ray diffraction and chemical composition analysis, resistivity and magnetic susceptibility on as grown sample, magnified figure of P variation of the Kondo resistance upturn, magnetoresistance at 15 GPa, $R(T)$ near T_c upon compresssion and decompression P, field and current variation of the resistance drop near SC Tc.
[35] S. Karmakar, High Press. Res. **33**, 381 (2013).
[36] M. B. Maple, Appl. Phys. **9**, 179 (1976).
[37] Y. Guo, J. Dai, J. Zhao, C. Wu, D. Li, L. Zhang, W. Ning, M. Tian, X. C. Zeng, and Y. Xie, Phys. Rev. Lett. **113**, 157202 (2014).
[38] C. S. Yadav and A. K. Rastogi, Solid State Commun. **150**, 648 (2010).
[39] G. V. Kamarchuk, A. V. Khotkevich, V. M. Bagatsky, V. G. Ivanov, P. Molinie, A. Leblanc, and E. Faulques, Phys. Rev. B **63**, 073107 (2001).
[40] S. Pal, K. Debnath, S. N. Gupta, L. Harnagea, D. V. S. Muthu, U. Waghmare, and A. K. Sood (unpublished).
[41] J. S. Schilling and W. B. Holzapfel, Phys. Rev. B **8**, 1216 (1973).
[42] H. Olijnyk, J. Crone, and E. Luscher, Z. Phys. B: Condens. Matter **43**, 299 (1981).